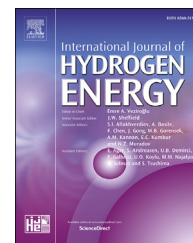


Available online at [www.sciencedirect.com](http://www.sciencedirect.com)

ScienceDirect

journal homepage: [www.elsevier.com/locate/ijhe](http://www.elsevier.com/locate/ijhe)

# SMC-DPC based active and reactive power control of grid-tied three phase inverter for PV systems

Harun Özbay <sup>a,\*</sup>, Selim Öncü <sup>b</sup>, Metin Kesler <sup>c</sup>

<sup>a</sup> Bilecik Seyh Edebali University Vocational High School, Bilecik, 11230, Turkey

<sup>b</sup> Karabük University Engineering Faculty, Karabük, 78050, Turkey

<sup>c</sup> Bilecik Seyh Edebali University Engineering Faculty, Bilecik, 11230, Turkey

## ARTICLE INFO

### Article history:

Received 12 November 2016

Received in revised form

1 March 2017

Accepted 4 April 2017

Available online 28 April 2017

### Keywords:

Maximum power point tracker (MPPT)

Sliding mode control (SMC)

Direct power control (DPC)

Grid-tied three phase inverter

Digital signal processor (DSP)

## ABSTRACT

In this paper, sliding mode control (SMC) – direct power controller (DPC) based active and reactive power controller for three-phase grid-tied photovoltaic (PV) system is proposed. The proposed system consists of two main controllers: the DC/DC boost converter to track the possible maximum power from the PV panels and the grid-tied three-phase inverter. The Perturb and Observe (P&O) algorithm is used to transfer the maximum power from the PV panels. Control of the active and reactive powers is performed using the SMC-DPC strategy without any rotating coordinate transformations or phase angle tracking of the grid voltage. In addition, extra current control cycles are not used to simplify the system design and to increase transient performance. The fixed switching frequency is obtained by using space vector modulation (SVM). The proposed system provides very good results both in transient and steady states with the simple algorithms of P&O and SMC-DPC methods. Moreover, the results are evaluated by comparing the SMC-DPC method developed for MPPT and the traditional PI control method. The proposed controller method is achieved with TMS320F28335 DSP processor and the system is experimentally tested for 12 kW PV generation systems.

© 2017 Hydrogen Energy Publications LLC. Published by Elsevier Ltd. All rights reserved.

## Introduction

There has been an increasing demand for natural resources as fossil fuels and energy depending on the increasing world population, industrialization and increasing production and trade facilities. Fossil fuels play an important role to meet the energy demand in the world and they seem to maintain their importance in the future. However, the need for renewable energy sources has been more apparent when considering the fact that fossil fuels will not meet the energy demand in the world with the limited known reserve amounts. Therefore,

Photovoltaic (PV) systems have been one of the most popular renewable energy sources [1,2]. Fossil-fuel power stations give negative effects on environmental. On the contrary, it has been found in recent years that the energy obtained from solar gives no negative effects on environmental. Therefore, this subject has gained more attention for the researchers [3].

PV systems are widely used in many fields such as grid-tied inverters, irrigation systems, farm houses, off-grid systems, space vehicles and military applications [4]. Although PV panels have many advantages in energy generation, the efficiency is very low depending on some environmental factors such as temperature, radiation level, shading and dirt.

\* Corresponding author.

E-mail address: [harun.ozbay@bilecik.edu.tr](mailto:harun.ozbay@bilecik.edu.tr) (H. Özbay).

<http://dx.doi.org/10.1016/j.ijhydene.2017.04.020>

0360-3199/© 2017 Hydrogen Energy Publications LLC. Published by Elsevier Ltd. All rights reserved.

Therefore, it is a crucial issue to transfer the maximum power from PV panels. Besides, a DC/DC boost converter is used between PV system and load to transfer the maximum possible power. The maximum power is obtained by operating the converter using power tracking algorithm [5,6]. There are many control algorithms for maximum power point tracker (MPPT). The most common control methods are Perturb & Observe (P&O) and Hill Climbing methods due to their simplicity, practicality and high efficiency [7]. Moreover, the most important advantage of these methods are that they are independent from PV characteristic, temperature and radiation level while tracking the maximum power point. As a result, maximum power point can be achieved more sensitively, which are important conditions for grid-tied inverter providing active/reactive power control [8].

In literature, there have been some studies on grid-tied inverters. While in some studies inverters are designed in a way to inject only active power to the grid, multi-functional grid-tied inverters are also examined [9,10]. The operating modes of the inverters obtained in the studies are as follows: (1) The available maximum active power providing mode (2) The reactive power providing mode depending on the voltage (3) The available maximum reactive power providing mode (4) The reactive power and power factor determination mode [11]. Grid-tied PV systems consist of a wide range of processes such as DC/DC conversion, maximum power tracking control, grid-tied inverter technology and the optimization of all factors. In addition, the studies on grid-tied three phase inverters have focused on a better performance, high efficiency and reliability. Many problems have been encountered during the development process and some new innovations have been found while solving the problems. In particular, grid-tied three phase inverters have gained importance due to the increase in renewable energy sources [12]. Therefore, these studies on the integration of the renewable energy sources with the grid-tied inverters have been gained more importance.

Moreover, in literature many studies have been focused on the control of grid-tied inverters. PI, PID or PR controllers are generally used to control the grid-tied inverters [13,14]. However, PI and PID controller cannot eliminate steady state error for sinusoidal signals. Although the PR controller has the ability to track sinusoidal signals without steady state errors, some deviation of the frequency of the selected harmonic component greatly disturbs the control performance [15]. Sliding mode control is an effective controller based on a variable structure control strategy developed to remove these negative effects in nonlinear systems. It has a robust control, simple application and fast response features under the exchange of all system parameters. However, when the system is under control, it can cause undesirable chattering in currents. Therefore, direct power control (DPC) using a sliding mode scheme has been proposed to remove this drawback [16]. The principle of the DPC method is inspired by a direct torque control (DTC) technique [17] applied to the drive systems of electrical machines. According to this principle the choice of transducer switching states is based on a predefined commutation table. The most significant disadvantage of this technique is the variable switching frequency, which produces an undesirable wide band gap harmonic spectrum

range. As a result, a sliding mode direct power control (SMC-DPC) with no extra current loop and low crackling level has been proposed [18].

This study presents the experimental results of a DSP based active and reactive power flow control algorithm for a grid-tied three-phase PV inverter. Maximum power transfer is achieved with DC/DC boost converter and P&O algorithm. In the proposed system, maximum power is tracked by DC/DC boost converter and the current injected to the grid is controlled by the three phase inverter. The controller adjusts the line current without exceeding limitations. Furthermore, the inverter can inject inductive or capacitive reactive power demanded by the grid. By doing this, the grid requirements are met by giving only reactive power support to the grid even when there is no solar radiation. All the controls in the designed system are achieved by TMS320F28335 DSP processor. System controller is tested and verified in PSIM software and the embedded code is generated in accordance with the DSP. The generated codes are compiled and loaded into the DSP. Therefore, the changes in the system or the control algorithm could be performed easily with the help of the embedded code generation. The control algorithm and the output power control of the system are carried out and the results are evaluated. The results show that the designed control system operates successfully and gives dynamic responses to the MPPT process and the system demands.

In the study, the proposed control algorithm is presented which combines the maximum power point tracker algorithm, direct power control strategy, sliding mode control approach and space vector modulation operating with a constant frequency. Therefore, a very dynamic controller is obtained which can arrange the active and reactive powers of the grid-tied PV inverter directly.

## Description and modeling of proposed system

### MPPT control algorithm

P&O is the most widely used MPPT techniques due to high accuracy at MPP [19–21]. In P&O method, PV panel power is calculated by measuring the PV voltage/current and compared with the previous one. The operating point of the converter is changed according to the power measurements. If the power increases, perturbation direction is not changed. Otherwise,

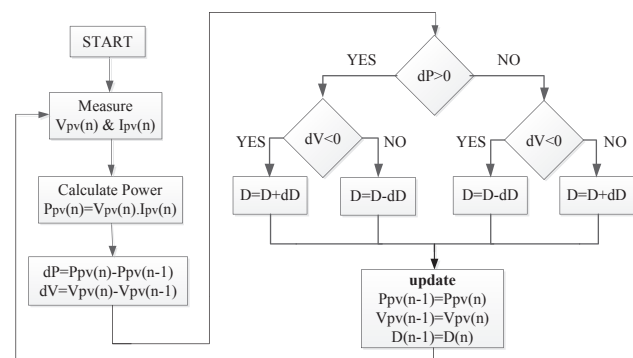


Fig. 1 – The flow chart of P&O method.

perturbation direction is reversed. This process will be applied until MPP is achieved [22]. The flow chart of the P&O algorithm is shown in Fig. 1.

Operating voltage of the PV system is changed with a small increase of  $\Delta V$ . Therefore,  $\Delta P$  is also changed. The power of the PV system is compared with the previous one. If the power is higher than the previous one ( $\Delta P > 0$ ) and the voltage of the PV system is higher than the previous one ( $\Delta V > 0$ ), the duty ratio is increased. If the voltage of the PV system is smaller than the previous one ( $\Delta V < 0$ ), the duty ratio is decreased. On the

other hand, if the power of the PV system is smaller than the previous one ( $\Delta P < 0$ ) and the voltage of the PV system is higher than the previous one ( $\Delta V > 0$ ), the duty ratio is decreased. However, if the voltage is smaller than the previous one ( $\Delta V < 0$ ) the duty ratio is increased.

Fig. 2 shows the used PV model characteristic under constant temperature (25 °C). As the solar radiation rises, the maximum available power increases. Therefore, it becomes important to transfer maximum available power from PV cells.

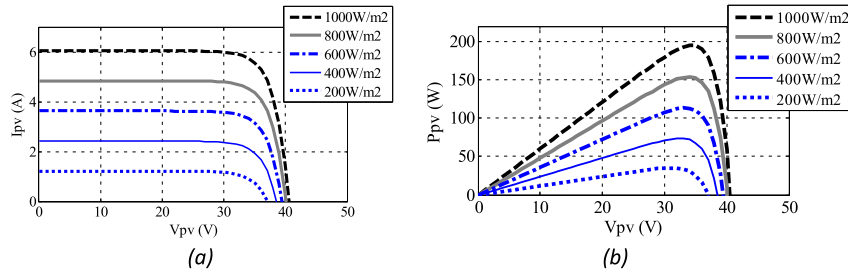


Fig. 2 – (a) I–V curves with varying irradiance (b) P–V curves with varying irradiance.

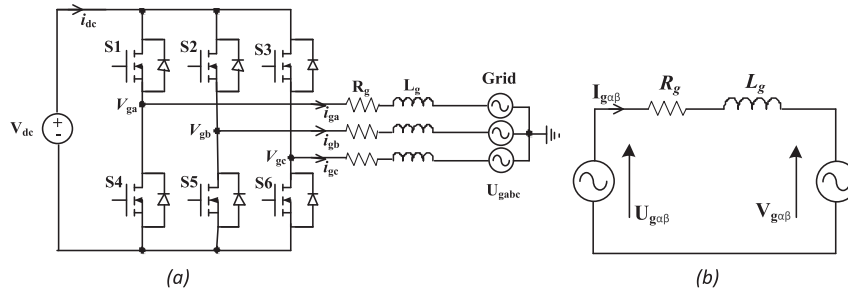


Fig. 3 – (a) The grid-tied three phase inverter (b) Equivalent circuit.

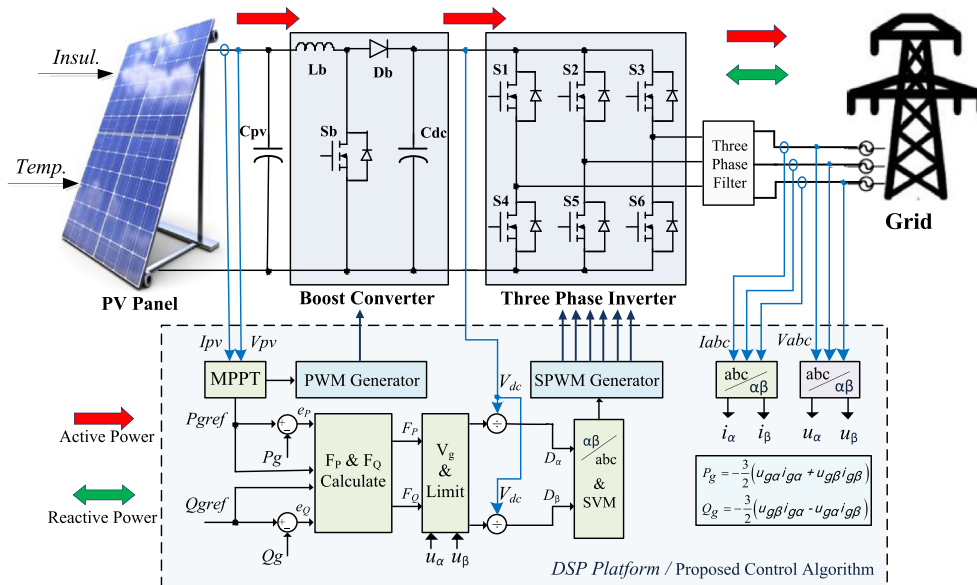


Fig. 4 – The block diagram of the proposed system.

Grid-tied inverter model

The grid-tied three phase inverter and equivalent circuit are shown in Fig. 3. The inverter consists of a DC voltage source ( $V_{dc}$ ), six power switches (S1–S6), line filter inductors ( $L_g$ ).

The relationship between the power supply, inverter voltage and line currents in the stationary reference frame according to Fig. 3 (a) is given as follows [23,24];

$$V_{g\alpha\beta} = R_g + I_g + L_g \frac{di_{g\alpha\beta}}{dt} + U_{g\alpha\beta} \tag{1}$$

The active and reactive power outputs on the network side can be defined for a balanced three-phase system as follows:

$$S_g = P_g + jQ_g = -\frac{3}{2} U_{g\alpha\beta} \times I_{g\alpha\beta}$$

$$P_g = -\frac{3}{2} (u_{g\alpha} i_{g\alpha} + u_{g\beta} i_{g\beta}) \tag{2}$$

$$Q_g = -\frac{3}{2} (u_{g\beta} i_{g\alpha} - u_{g\alpha} i_{g\beta})$$

The derivations of instantaneous active and reactive power changes can be described as follows;

$$\frac{dP_g}{dt} = -\frac{3}{2} \left( u_{g\alpha} \frac{di_{g\alpha}}{dt} + i_{g\alpha} \frac{du_{g\alpha}}{dt} + u_{g\beta} \frac{di_{g\beta}}{dt} + i_{g\beta} \frac{du_{g\beta}}{dt} \right) \tag{3}$$

$$\frac{dQ_g}{dt} = -\frac{3}{2} \left( u_{g\beta} \frac{di_{g\alpha}}{dt} + i_{g\alpha} \frac{du_{g\beta}}{dt} - u_{g\beta} \frac{di_{g\beta}}{dt} - i_{g\beta} \frac{du_{g\alpha}}{dt} \right)$$

According to Equation (1), the  $\alpha, \beta$  components of the instantaneous changes in currents can be expressed as follows;

$$\frac{di_{g\alpha}}{dt} = \frac{1}{L_g} (u_{g\alpha} - R_g i_{g\alpha} - v_{g\alpha}) \tag{4}$$

$$\frac{di_{g\beta}}{dt} = \frac{1}{L_g} (u_{g\beta} - R_g i_{g\beta} - v_{g\beta})$$

As a result, the obtained following equations can be used to design the proposed direct power control technique.

$$\frac{dP_g}{dt} = -\frac{3}{2L_g} \left( (u_{g\alpha}^2 + u_{g\beta}^2) - (u_{g\alpha} v_{g\alpha} + u_{g\beta} v_{g\beta}) \right) - \frac{R_g}{L_g} P_g - \omega_g Q_g \tag{5}$$

$$\frac{dQ_g}{dt} = -\frac{3}{2L_g} (u_{g\alpha} v_{g\beta} + u_{g\beta} v_{g\alpha}) - \frac{R_g}{L_g} Q_g + \omega_g P_g$$

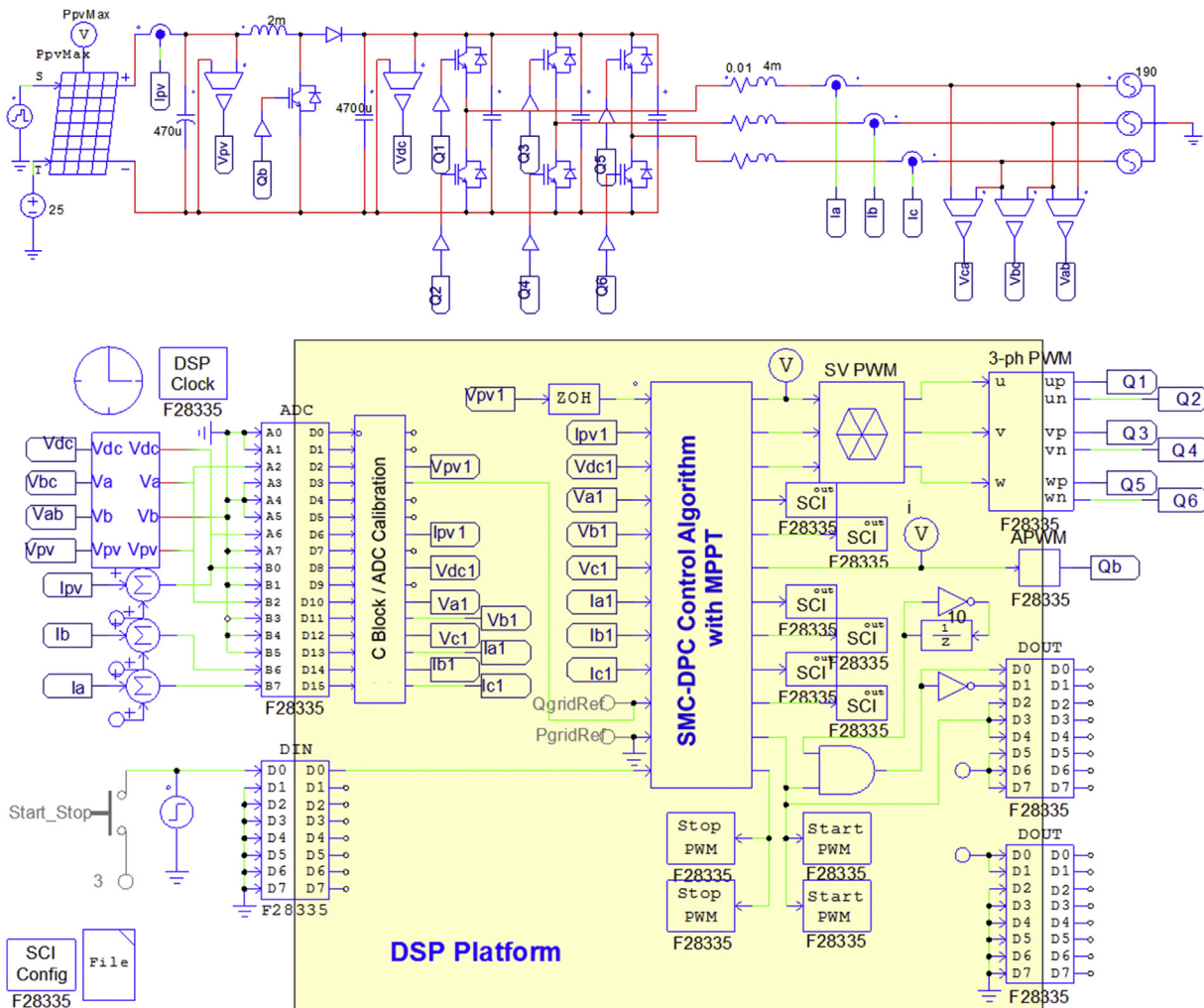


Fig. 5 – PSIM circuit of the proposed system and embedded code generation method.

### Proposed SMC-DPC based model for PV system

The overall block diagram of the proposed system consisting of the PV generator, the MPPT control algorithm, the SMC-DPC control algorithm, the DC/DC boost converter and the three phase inverter are shown in Fig. 4.

In the proposed system, total 63 PV panel arrays (nine series arrays and then seven parallel arrays) are connected and 325 V is obtained from these panels. In order to achieve MPPT, PV voltage is increased by the boost converter and applied to three phase inverter. The converter and the inverter are controlled at 10 kHz. In the proposed system the

**Table 1 – The parameters of the proposed system.**

Parameters	Values
Maximum PV power (KW)	12
PV input capacitor ( $\mu\text{F}$ )	470
Boost inductor (mH)	2.0
Boost capacitor ( $\mu\text{F}$ )	4700
Filter resistance (m ohms)	10
Filter inductance (mH)	4.0
Line to line rms voltage (V)	190
AC supply frequency (Hz)	50

**Table 2 – Control Parameters of the proposed SMC-DPC.**

Parameters	Values
Positive gains $K_p$ and $K_Q$	3000
Control gains $K_{p1}$ and $K_{Q1}$	$10^5$
Width of boundary layer $\delta_p$ and $\delta_Q$	50, 100

controller is simulated in PSIM software and is based on embedded code generation in C language for TMS320F28335 DSP processor. PV and grid current/voltage values are measured by sensors and transmitted to DSP in order to calculate the instantaneous active and reactive powers. With the proposed SMC-DPC with MPPT algorithms, DSP generates directly inverter voltage reference in the stationary reference frame according to active and reactive power errors. Control of the nonlinear systems having time-varying parameters and complex dynamics is more difficult compared to the classical controllers. SMC is an effective control method in the control of such systems. The purpose of applying the SMC method to closed-loop control systems is to send the error to the sliding surface or, alternatively, to the switching surface and to hold the error on this surface. For DC/AC inverters, the control targets are to track or slide along the predefined active and reactive power trajectory. For a good transient response and minimum steady-state error, the switching surfaces can be integral and can be defined as follows [16];

$$S_p = e_p(t) + K_p \int_0^t e_p(\tau) d\tau - e_p(0) \quad (6)$$

$$S_Q = e_Q(t) + K_Q \int_0^t e_Q(\tau) d\tau - e_Q(0)$$

where  $e_p = P_{gref} - P_g$  ve  $e_Q = Q_{gref} - Q_g$  are the errors between reference values and instantaneous actual values of active and reactive powers.  $K_p$  and  $K_Q$  positive control gains.  $S_p = 0$  and  $S_Q = 0$  manifold states show that the active and reactive powers of the inverter are precisely monitored. As a result, sufficient condition for the formation of sliding mode can be derived from the following equations;

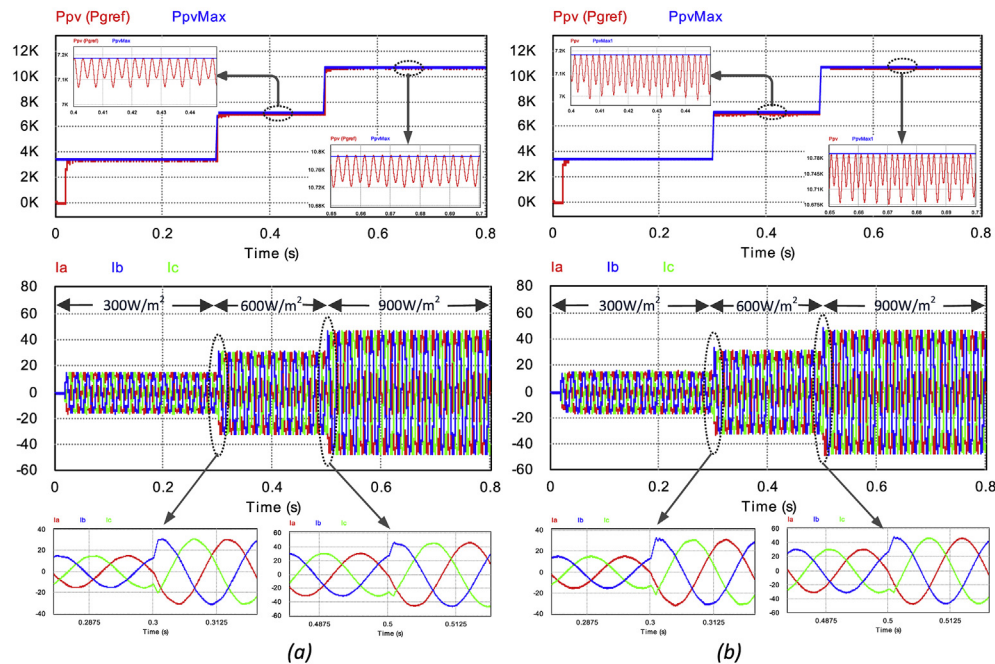


**Fig. 6 – Simulation results of maximum power tracking under 300–600–900 W/m<sup>2</sup> solar radiation. (a) Proposed SMC-DPC with P&O algorithm (b) Conventional controller with P&O algorithm [25].**

$$\begin{aligned} \frac{de_P(t)}{dt} &= -K_P e_P(t) \\ \frac{de_Q(t)}{dt} &= -K_Q e_Q(t) \end{aligned} \tag{7}$$

The aim of designing SMC law in the proposed system is to force the system trajectory to the switching surface interaction in order to generate inverter output voltage reference. This can be obtained by deriving Equation (6);

$$\begin{aligned} \frac{dS_P}{dt} &= \frac{de_P(t)}{dt} + K_P e_P(t) = -\frac{d}{dt} P_g + K_P (P_{gref} - P_g) \\ \frac{dS_Q}{dt} &= \frac{de_Q(t)}{dt} + K_Q e_Q(t) = -\frac{d}{dt} Q_g + K_Q (Q_{gref} - Q_g) \end{aligned} \tag{8}$$

When Equation (5) is substituted in the obtained equation;

$$\frac{dS}{dt} = F + DV_g \tag{9}$$

where;  $F = [F_P \ F_Q]^T$   $V_g = [v_{g\alpha} \ v_{g\beta}]^T$   $D = -\frac{3}{2L_g} \begin{bmatrix} u_{g\alpha} & u_{g\beta} \\ u_{g\beta} & -u_{g\alpha} \end{bmatrix}^T$

$F_P$  and  $F_Q$  values are expressed as follows;

$$\begin{aligned} F_P &= \frac{3}{2L_g} (u_{g\alpha}^2 + u_{g\beta}^2) - \frac{R_g}{L_g} P_g - \omega_g Q_g + K_P (P_{gref} - P_g) \\ F_Q &= \frac{R_g}{L_g} Q_g - \omega_g P_g + K_Q (Q_{gref} - Q_g) \end{aligned} \tag{10}$$

Quadratic Lyapunov function must be chosen as follows;

$$W = \frac{1}{2} S^T S \tag{11}$$

The time derivative of Quadratic Lyapunov function is as follows:

$$\frac{dW}{dt} = S^T \frac{dS}{dt} = S^T (F + DV_g) \tag{12}$$

When the  $S \neq 0$ , the switch control law the derivative of  $W$  must be chosen as correctly as to be negative:

$$V_g = -D^{-1} \left\{ \begin{bmatrix} F_P \\ F_Q \end{bmatrix} + \begin{bmatrix} K_{P1} & 0 \\ 0 & K_{Q1} \end{bmatrix} \begin{bmatrix} \text{sgn}(S_P) \\ \text{sgn}(S_Q) \end{bmatrix} \right\} \tag{13}$$

The instantaneous active and reactive powers in the grid-tied inverters are tracked quickly by SMC method. However, fast switching can produce unexpected chattering. This situation has an undesired effect since it can cause unpredictable instability. In order to remove this drawback, the discontinuous part of the controller is softened by using a boundary layer around the sliding surface. As a result, the continuous function around the sliding surface is as follows;

$$\text{sgn}(S_j) = \begin{cases} 1, & \text{if } S_j > \delta_j \\ \frac{S_j}{\delta_j}, & \text{if } |S_j| \leq \delta_j \\ -1, & \text{if } S_j < -\delta_j \end{cases} \tag{14}$$

where  $\delta > 0$  represents the width of the boundary layer,  $j$  represents the active and reactive power. Thus, using Equations (10) and (14), the voltage reference of the inverter at the stationary reference frame is obtained and transferred to the SVM module to generate the required switching voltage vectors and durations.

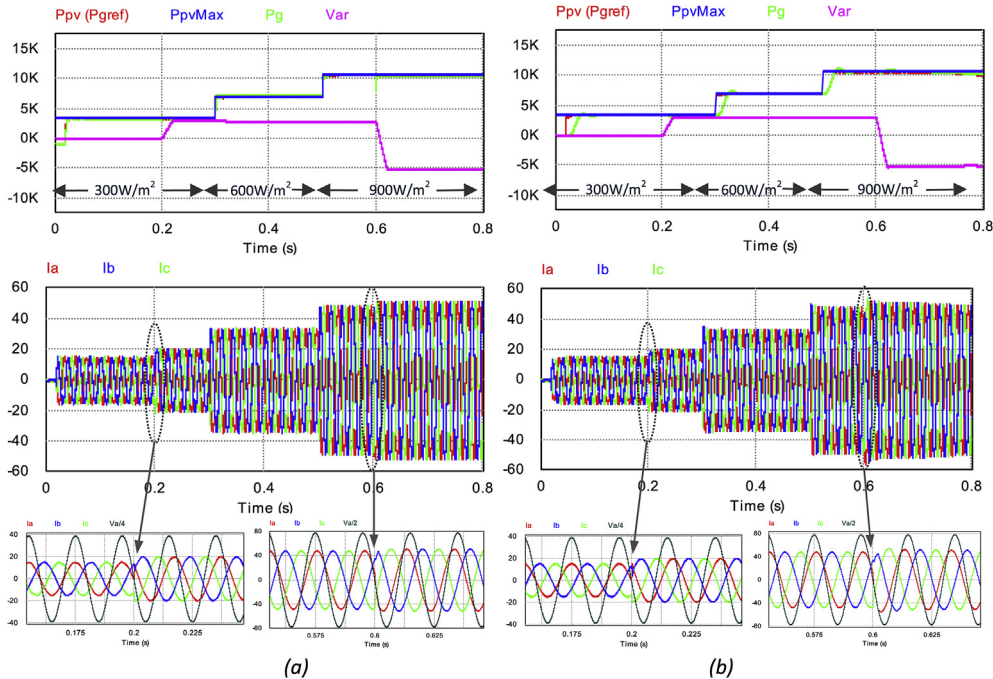


Fig. 7 – Verification of the proposed controllers using PSIM for various solar radiation and various  $Q_{gref}$ . (a) Proposed SMC-DPC with P&O algorithm (b) Conventional controller with P&O algorithm [25].

### PSIM simulation results and embedded code generation

In order to verify the performance of the proposed SMC-DPC method, simulation studies are performed with PSIM software. The obtained results are compared with the conventional controller system [25]. The simulation step durations are adjusted as  $1 \mu\text{s}$ . The switching frequency is adjusted as 10 kHz, dead time  $2 \mu\text{s}$ . However, the sampling frequency is selected as 40 kHz to increase the system performance. Moreover, the embedded code generation is provided for TMS320F28335 DSP controller using PSIM program. Therefore the application procedure has gained practicality. The PSIM schema of the proposed system is given in Fig. 5. The parameters of the simulation model and the applied system are given in Table 1. The control parameters for the proposed SMC-DPC method are listed in Table 2.

Solar radiation varies throughout the day. Simulation results carried out at 300–600–900  $\text{W/m}^2$  solar radiation levels

are shown in Fig. 6. Duty cycle of the boost converter is changed between 10 and 70% to track the MPP at 10 kHz. Therefore, the maximum power extracted from PV panels even during the rapid climate changes is tracked by P&O MPPT algorithm. The algorithm also generates  $P_{\text{gref}}$  reference for three phase inverter. The results obtained from the proposed SMC-DPC method and the results of the conventional PI controlled method obtained from the previous study are given in Fig. 6 (a) and (b), respectively. As can be seen from Fig. 6, since the proposed SMC-DPC method can perform the instantaneous power control directly, less oscillation occur compared to conventional PI controller. In addition, SMC-DPC method, which is recommended for instantaneous power changes, makes the transition of the currents transferred to the grid more dynamic.

In the active and reactive power test scenario, at time 20 ms, the PWM generator is started with  $300 \text{ W/m}^2$  solar radiation. At time 200 ms, the  $Q_{\text{gref}}$  is rapidly changed from 0 to 3000 VAR lagging (inductive) reactive power. At time 300 ms, the solar radiation is rapidly changed from 300 to  $600 \text{ W/m}^2$ . At

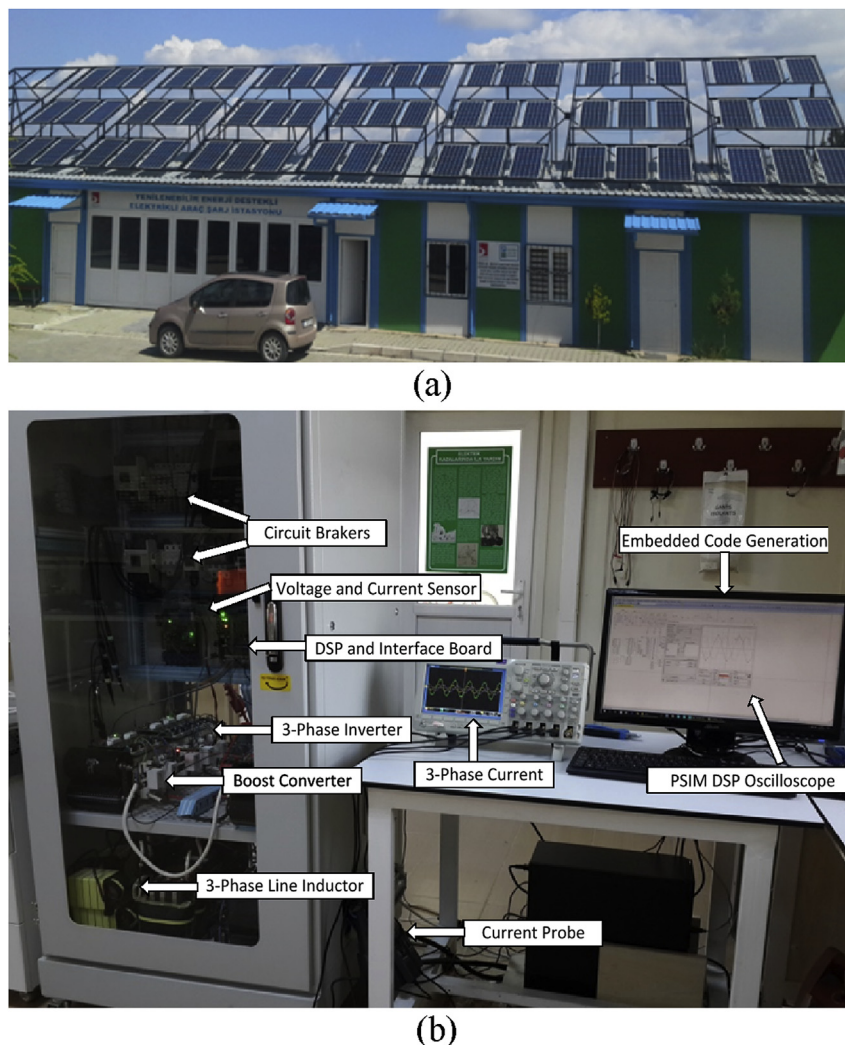


Fig. 8 – (a) The PV panel arrays (b) Experimental setup of proposed system.

time 500 ms, the solar radiation is rapidly changed from 600 to 900 W/m<sup>2</sup>. Finally at time 600 ms, the  $Q_{\text{gref}}$  is rapidly changed from 3000 to -5000 VAR leading (capacitive) reactive power. Although the active and reactive power transient responses of both proposed and conventional controllers occurred in as short a few milliseconds, the proposed SMC-DPC controller has better steady-state during power changes. The related simulation results are shown in Fig. 7.

### Experimental study

In this study, nine series arrays and then seven parallel arrays connected PV panel arrays are used. The PV panels parameters are as follows:  $V_{\text{mp}} = 36$  V,  $I_{\text{mp}} = 5.28$  A and 190 W output power. The panels are installed at 40° tilt angle at Bilecik Seyh Edebali University, Centre Campus and three phase grid tied inverter is designed and implemented. Fig. 8 (a) and (b) shows the PV generation system and the experimental setup of the proposed converter/inverter respectively. The system is detail obtained when the power extracted from PV panels is transferred to the grid by the three phase inverter.

MPPT and the grid-tied three phase inverter are controlled with TMS320F28335 DSP. Both the boost converter and the three phase inverter outputs are limited to prevent the damage on the circuits. To measure line voltage and current, voltage and current sensors are used. The isolation of the inverter is required for the system safety. Therefore, in system 190/380 V three phase transformer is used to isolate the inverter form the grid. P&O MPPT algorithm is used for the experimental study. The currents transferred to the grid and the voltage of the A phase are measured. The experimental study results are obtained under 720 W/m<sup>2</sup> solar radiation level. Approximately 8.5 kW power is obtained from PV panels and transferred to the three phase grid successfully. Reactive power support is provided in achieving MPPT as in simulation studies. Fig. 9 shows the 8.5 kW maximum power command of PV panels and the currents obtained when 3 kVAR and -5 kVAR reactive power command is supplied.

When the reactive power command is given to the system, the currents have a soft transient and the system has fast steady state response. 3 kVAR & -5 kVAR reactive power and 8.5 kW active power are transferred to the grid in a way that the total power extracted from PV panels will stay stable. Therefore, the proposed system performs the inductive and capacitive power supports successfully while the active power is transferred to the grid. If the apparent power injected to the grid is needed limit for inverter safety, the algorithm can be run without the MPPT. Thus, the power obtained from the PV panel is regarded as apparent power and is equal to the sum of the active power and the reactive power. The experimental study results of constant apparent power are obtained under 950 W/m<sup>2</sup> solar radiation level. Approximately 11.4 kW power is obtained from PV panels and transferred to the three phase grid successfully. Fig. 10 shows the 11.4 kVA maximum apparent power command of PV panels and the currents obtained when 3 kVAR and -5 kVAR reactive power command is supplied.

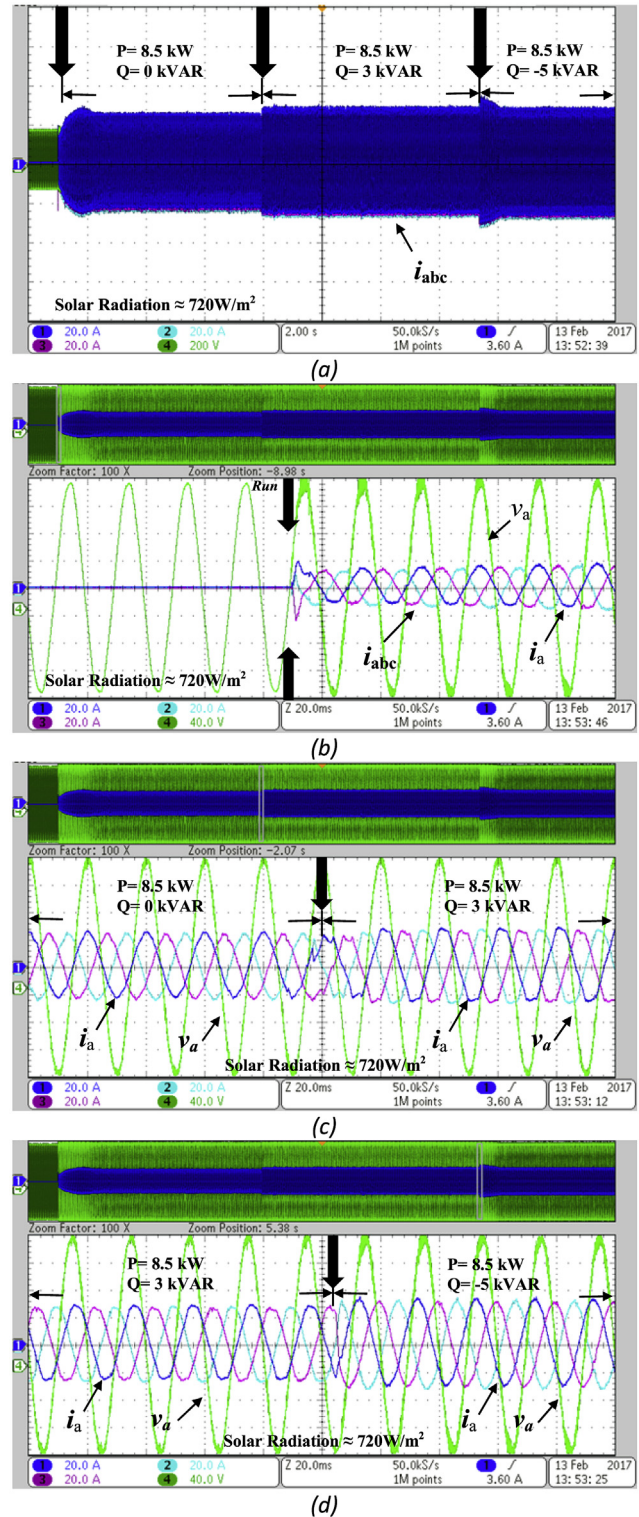
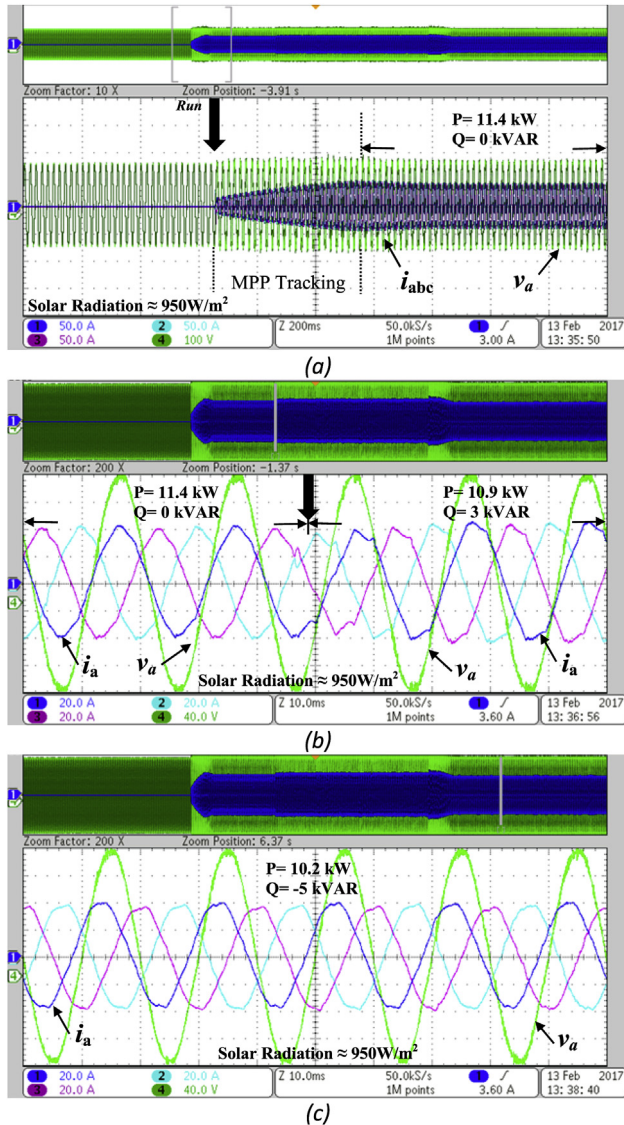


Fig. 9 – Experimental results of the proposed system for  $P = 8.5$  kW,  $SR = 720$  W/m<sup>2</sup>. (a) Transition from the active to reactive power operations (b) MPPT startup (c)  $Q_{\text{gref}} = 3$  kVAR. (d) Transition from the 3 kVAR inductive to -5 kVAR capacitive reactive power operations.



**Fig. 10** – Experimental results for the inverter in safe mode when over current without MPPT,  $S = 11.4 \text{ kVA}$ . (a) MPP tracking under  $950 \text{ W/m}^2$  solar radiation (b)  $P_{\text{gref}} = 10.9 \text{ kW}$ ,  $Q_{\text{gref}} = 3 \text{ kVAR}$ . (c)  $P_{\text{gref}} = 10.2 \text{ kW}$ ,  $Q_{\text{gref}} = -5 \text{ kVAR}$ .

## Conclusions

In this study SMC-DPC based active and reactive power flow control algorithm is proposed for grid-tied three-phase PV inverter system. In proposed system maximum available power is transferred from PV panels to the grid using MPPT algorithm. The proposed controller also receives an active power command ( $P_{\text{gref}}$ ) from the MPPT algorithm. Furthermore, if it is necessary, the utility grid sends a reactive power command. The proposed SMC-DPC method provides directly power control of the grid-tied inverter for PV systems. When the conventional and proposed method are compared under transient and steady-state conditions for the active and reactive power operation, the proposed controller has good response time and very stable in steady-state conditions. In

the proposed SMC-DPC method, the processing load of the DSP processor is reduced since the rotational coordinate transformation and the angular information of the mains voltage are no required. Therefore, since the operations are faster, the harmonics are adjusted to the standards by reducing the chattering of the currents transferred to the network. The proposed system is also suitable for battery chargers, hydrogen generation since it has high current control capability from grid or PV system.

According to the experimental results, the proposed system is quite suitable for active power and reactive power tuning capacity. Moreover, the proposed system has soft transition and fast response to MPPT control. The performance of the proposed control method is experimentally carried out for different active/reactive powers and at  $720 \text{ W/m}^2$  and  $950 \text{ W/m}^2$  radiation level. The obtained active power from PV panels transferred to the three phase grid successfully by the proposed system. An experimental setup is developed for the proposed system and it was operated at  $3 \text{ kVAR}$  inductive and  $-5 \text{ kVAR}$  capacitive reactive power while  $8.5 \text{ kW}$  power is transferred from PV panels. Furthermore, the experimental setup was operated at  $11.4 \text{ kVA}$  maximum apparent power obtained from PV panels to protect the inverter at power limits. During this time it was operated at  $10.2 \text{ kW}$  active power,  $-5 \text{ kVAR}$  reactive power and  $10.9 \text{ kW}$  active power,  $3 \text{ kVAR}$  reactive power. The proposed system controller responds to the commands of active power and reactive power in less than  $2 \text{ ms}$  time. Consequently, this paper has shown that a grid-tied three phase inverter for PV system is a candidate for reactive power support to utility grid.

## Acknowledgements

This research was supported by TUBITAK Research Fund (No: 115E104) and Karabuk University Research Fund (No: 14/2-DR-017).

## REFERENCES

- [1] Bose BK. Global warming: energy, environmental pollution, and the impact of power electronics. *IEEE Ind Electron Mag* 2010;4(1):6–17. Mar.
- [2] Turkyay Yavuz, Ibrahim Acar H. A solar domestic hot water system simulation study in Sivas, Turkey. *J Polytech* 2004;7.1.
- [3] Duz Hasan. Storing solar energy inside compressed air through a heat machine mechanism. *Gazi Univ J Sci* 2016;29.2:245–51.
- [4] Sick Friedrich, Erge Thomas. *Photovoltaics in buildings: a design handbook for architects and engineers*. Earthscan; 1996.
- [5] Li X, Wen H, Jiang L, Hu Y, Zhao C. An improved beta method with autoscoping factor for photovoltaic system. *IEEE Trans Ind Appl* 2016;52(5):4281–91.
- [6] Özbay H, Karafil A, Öncü S, Kesler M. DSP controlled high frequency battery charger for PV generation systems. In: *III. European Conference on Renewable Energy Systems (ECRES)*; 2015.
- [7] Ramulu C, Sanjeevikumar P, Karampuri R, Jain S, Ertas AH, Fedak V. A solar PV water pumping solution using a three-

- level cascaded inverter connected induction motor drive. *Eng Sci Technol Int J* 2016;19(4):1731–41.
- [8] ESRAM T, Chapman PL. Comparison of photovoltaic array maximum power point tracking techniques. *IEEE Trans Energy Convers EC* 2007;22(2):439.
- [9] Cagnano A, De Tuglie E, Liserre M, Mastromauro RA. Online optimal reactive power control strategy of PV inverters. *IEEE Trans Ind Electron* 2011;58(10):4549–58.
- [10] Balathandayuthapani S, Edrington CS, Henry SD, Cao J. Analysis and control of a photovoltaic system: application to a high-penetration case study. *IEEE Syst J* 2012;6(2):213–9.
- [11] Gonzalez S, Neely J, Ropp M. Effect of non-unity power factor operation in photovoltaic inverters employing grid support functions. In: *IEEE 40th photovoltaic specialist Conference*; 2014. p. 1498–503. 8–13 June.
- [12] Wu L, Zhao Z, Liu J. Intelligent controller for solar lighting system. *Tsinghua Univ J* 2003;43(9):1195–8.
- [13] Kesler M, Kisacikoglu MC, Tolbert LM. Vehicle-to-grid reactive power operation using plug-in electric vehicle bidirectional offboard charger. *Ind Electron IEEE Trans* 2014;61(12):6778–84.
- [14] Blaabjerg F, Teodorescu R, Liserre M, Timbus AV. Overview of control and grid synchronization for distributed power generation systems. *IEEE Trans Ind Electron* 2006;53(5):1398–409.
- [15] Chen Z, Luo A, Wang H, Chen Y, Li M, Huang Y. Adaptive sliding-mode voltage control for inverter operating in islanded mode in microgrid. *Int J Electr Power Energy Syst* 2015;66:133–43.
- [16] Hu J, Shang L, He Y, Zhu ZQ. Direct active and reactive power regulation of grid-connected DC/AC converters using sliding mode control approach. *IEEE Trans Power Electron* 2011;26(1):210–22.
- [17] Buja GS, Kazmierkowski MP. Direct torque control of PWM inverter-fed AC motors – a survey. *Ind Electron IEEE Trans* 2004;51:744–57.
- [18] Jeong HG, Kim WS, Lee KB, Jeong BC, Song SH. A sliding-mode approach to control the active and reactive powers for a DFIG in wind turbines. In: *Proc. IEEE Power Electron. Spec. Conf. 2008 (PESC 2008)*; 2008. p. 120–5.
- [19] Tafticht T, Agbossou K, Doumbia ML, Ché riti A. An improved maximum power point tracking method for photovoltaic systems. *Renew Energy* 2008;33:1508–16.
- [20] Maammeur H, Hamidat A, Loukarfi L. A numerical resolution of the current-voltage equation for a real photovoltaic cell. *Energy Proc* 2013;36:1212–21.
- [21] Ozdemir Saban, Altin Necmi, Sefa Ibrahim. Single stage three level grid interactive MPPT inverter for PV systems. *Energy Convers Manag* 2014;80:561–72.
- [22] Oncu Selim, Nacar Salih. Soft switching maximum power point tracker with resonant switch in PV system. *Int J Hydrogen Energy* 2016;41(29):12477–84.
- [23] Skvarenina Timothy L, editor. *The power electronics handbook*. CRC Press; 2001.
- [24] Jain Chinmay, Singh Bhim. A three-phase grid tied SPV system with adaptive DC link voltage for CPI voltage variations. *IEEE Trans Sustain Energy* 2016;7(1):337–44.
- [25] Özbay H, Öncü S, Kesler M. Active and reactive power control of grid-tied three phase inverter for PV systems. In: *IV. European Conference on Renewable Energy Systems (ECRES)*; 2016.